Effects of neutron exposure on the embryonic development of European sea bass (Dicentrarchus labrax), a candidate fish species for space aquaculture: simulated conditions on the ISS and during a lunar mission

Cyrille Przybyla, Richard Babut, Hugo Laganier, Gilbert Dutto, Emmanuel Mansuy, Sarah Elie, Stéphane Lallement, Isabelle Cavalie, Maria J Darias, Sophie Hermet, et al.

frontiers | Frontiers in Space Technologies

TYPE Original Research
PUBLISHED 16 April 2025
DOI 10.3389/frspt.2025.1571592

OPEN ACCESS

EDITED BY
Antonio Mattia Grande,
Polytechnic University of Milan, Italy

REVIEWED BY
T. John Tharakan,
Indian Space Research Organisation, India
Marta Monteiro,
University of Aveiro, Portugal

*CORRESPONDENCE
Cyrille Przybyla,
Cyrille.przybyla@ifremer.fr
Christelle Adam-Guillermin,
christelle.adam-guillermin@asnr.fr

RECEIVED 05 February 2025
ACCEPTED 25 March 2025
PUBLISHED 16 April 2025

CITATION
Przybyla C, Babut R, Laganier H, Dutto G, Mansuy E, Elie S, Lallement S, Cavalie I, Darias MJ, Hermet S, Balcon N, Perrot Y and Adam-Guillermin C (2025) Effects of neutron exposure on the embryonic development of European sea bass (*Dicentrarchus labrax*), a candidate fish species for space aquaculture: simulated conditions on the ISS and during a lunar mission.
Front. Space Technol. 6:1571592.
doi: 10.3389/frspt.2025.1571592

Effects of neutron exposure on the embryonic development of European sea bass (*Dicentrarchus labrax*), a candidate fish species for space aquaculture: simulated conditions on the ISS and during a lunar mission

Cyrille Przybyla[1]*, Richard Babut[2], Hugo Laganier[1], Gilbert Dutto[1], Emmanuel Mansuy[1], Sarah Elie[2], Stéphane Lallement[1], Isabelle Cavalie[3], Maria J. Darias[4], Sophie Hermet[4], Nicolas Balcon[5], Yann Perrot[6] and Christelle Adam-Guillermin[2]*

[1]MARBEC, Univ Montpellier CNRS, Ifremer, IRD, Palavas-les-Flots, France, [2]Autorité de Sûreté Nucléaire et de Radioprotection (ASNR), PSE-SANTE/SDOS/LMDN, Saint-Paul-Lez-Durance, France, [3]Autorité de Sûreté Nucléaire et de Radioprotection (ASNR), PSE-ENV/SERPEN/LECO, Saint-Paul-Lez-Durance, France, [4]MARBEC, Univ Montpellier, CNRS, Ifremer, IRD, Montpellier, France, [5]French National Space Agency (CNES), Toulouse, France, [6]Autorité de Sûreté Nucléaire et de Radioprotection (ASNR), PSE-SANTE/SDOS/LDRI, Fontenay-aux-Roses, France

One of the scenarios for manned space exploration involves the presence of a community on a lunar base that is partially autonomous in terms of food production. Space aquaculture could represent a source of nutrient-rich food to supplement the supply of photosynthetic organisms. To assess the feasibility of safely transporting aquaculture fish embryos to the Moon, the impact of secondary particles produced by cosmic radiation within the space vehicle cabin on fish embryogenesis and DNA damage was evaluated. Among these secondary particles this study focuses on neutron which is one the most hazardous radiation for living organisms. Using a particle accelerator, European sea bass (*Dicentrarchus labrax*) eggs were irradiated with neutrons at two dose rates, representative of International Space Station (ISS) and lunar missions. The mean absorbed dose rates in fish eggs were 16.7 μGy h^{-1} (total dose of 0.57 mGy) and 585 μGy h^{-1} (total dose of 12 mGy) for the ISS and lunar mission simulations, respectively. Hatching rate, histology and DNA integrity (assessed by alkaline comet assay) of fish larvae were evaluated for both neutron dose rates. Genotoxicity results showed DNA alterations in newly hatched larvae after 48 and 72 h of exposure. However, no modifications in hatching rate or histological structure of the exposed larvae were observed at either dose rate. Although further long-term studies are needed to verify their potential for

"off-Earth food production," these results complement previous experiments and confirm the hatchability of an aquaculture species under neutron exposure conditions of an ISS or lunar mission.

KEYWORDS

space aquaculture, neutron, ISS, Moon, European sea bass

1 Introduction

Over the last decade, major space-faring nations have been considering space exploration programs that include medium- and long-term manned stays outside our planet, notably on the Moon. While several technological challenges still need to be addressed, such as the supply of energy and oxygen or the construction of the base, the recycling of biological waste and the nutrition of crews are central concerns (Verseux et al., 2022). Economic constraints and industrial realities drastically reduce the potential for cargo rotation between the Earth and the Moon to provide food. Moreover, the storage of freeze-dried food is unstable, especially concerning essential nutrients such as potassium, calcium and vitamins, with vitamins A, C, B1 and B6 being the most sensitive to storage degradation after 1 year (Cooper et al., 2017). Unstable micronutrients also include vitamins D and K, which are critical for muscle and bone maintenance in altered gravity.

One of the major objectives of a bioregenerative life-support system is to provide fresh food sources for crewed missions (in addition to food delivered by cargo) using *in situ* resources and converting molecules from the biological waste streams into edible food biomass. Much research has focused on the growth and production of photosynthetic organisms in altered gravity, such as plants, vegetables (Verseux et al., 2022) and microalgae (Zabel et al., 2016). In addition to these photosynthetic sources already studied and considered in a lunar greenhouse (Zeidler et al., 2017), space aquaculture production at a Moon base could be a promising way to complete the nutritional requirements of lunar residents. Furthermore, astronauts on International Space Station (ISS) missions report that deliveries of fresh food provide profound psychological benefits. Beyond nutritional uptake, the diversity of farmed aquatic species and their different tastes could have a positive psychological impact on the crew and help avoid menu fatigue in a remote environment (Douglas et al., 2020).

The Lunar Hatch program, supported by the French Space Agency (CNES) and the French Institute for Ocean Science (Ifremer), is investigating the feasibility of developing space aquaculture by studying the viability of fish embryos sent from the Earth to the Moon. The main growth period of the fish would occur on the Moon, where they would be reared in a recirculating aquaculture system until they reach an edible size (Przybyla, 2021). The first step of this program is to study the impact of the Moon journey environment on aquaculture fish embryos and assess the viability of the organisms once they arrive at the lunar base. In aquaculture hatcheries or in nature, the embryogenesis of fish takes place in calm conditions. The influence of vibrations during launch (Przybyla et al., 2020), the hypergravity induced by rocket acceleration and the simulated microgravity have already been studied. Results show the continuity of embryogenesis until hatching in these uncommon situations. The hatching rates of exposed groups were not significantly different from those of the control groups, regardless of the situation. Moreover, stress and oxygen consumption in simulated microgravity were at the same levels as in an Earth environment (Przybyla et al., 2023).

In addition to these physical factors encountered in space, cosmic radiation may impact fish embryo viability. During the journey to the Moon, the shielded spacecraft structure is exposed to different sources of ionizing radiation: radiation "belts" in the near-Earth environment, which contain mostly energetic "trapped" protons and electrons; galactic cosmic radiation (GCR), composed of energetic protons, He nuclei and heavy ions of nuclear charge up to ^{26}Fe and higher; and solar particle events (SPE), formed of solar protons and heavier ions accelerated by eruptive phenomena such as coronal mass ejections or directional "solar flares" (Shavers et al., 2024). Unlike most SPE particles, which can be stopped by adequate shielding, GCR particles penetrate the spacecraft and other surfaces, producing secondary particles, including neutrons, lighter nuclei, electrons and γ rays (Warden and Bayazitoglu, 2019), inside the habitable section, where the aquaculture fish embryos will be located during the flight. These secondary emissions carry the high energy transferred from the initial incident particle through shielding materials and have the potential to damage critical cellular components when passing through the tissues of living organisms (Chancellor et al., 2018).

This paper focuses on a secondary neutron exposure. Indeed, neutrons are considered highly carcinogenic and far more effective in inducing biological damage than low linear energy transfer radiation in humans (Fisher et al., 2020). In fish embryos, neutrons are also far more effective in inducing biological effects than γ radiation (Hyodo-Taguchi et al., 1973; Kuhne et al., 2009), making them biologically priority particles to study in the context of the exposure of aquaculture fish eggs to secondary particles in the cabin of the space vehicle during a lunar trajectory.

There is a lack of knowledge on the effect of neutrons on aquaculture fish, but data have been published on fish model species. Exposure of medaka (*Oryzias latipes*) embryos at different developmental stages to increasing absorbed doses of neutrons up to 80 Gy (dose rate of 5.4 10^{7} μGy h^{-1}, average energy of 2 MeV) demonstrated that the hatching rate, mortality and malformations depend on the intensity of exposure. Hatchability was reduced by 50% at 2.25–35 Gy, depending on the developmental stage, while malformations were observed above

Abbreviations: DSBs, Double-strand breaks; GCR, Galactic cosmic rays; Gy Gray, unit of radiation dose; Hpf, Hours post-fertilization; ISS, International Space Station; LET, Linear energy transfer; MeV, Mega electron-volt, measure of kinetic energy of 10^{6} electron-volt; Sv Sievert, unit of dose equivalent (the biological effect of ionization radiation); SPE, Solar particle events; SSBs, Single-strand breaks; °C, Degree Celsius.

2 Gy. Fish embryos appeared to be more resistant to neutrons once the outline of the caudal fin had formed, suggesting robustness linked to critical mass and resistance capability. As often described, hatching times also differ from expectations. Early irradiation appears to induce a prolongation of embryogenesis, while later irradiation accelerates hatching (Hyodo-Taguchi et al., 1973).

Still for the medaka, the effects of neutrons with differential energy spreads ranging from 1 to 800 MeV were also measured *in vivo* (Kuhne et al., 2009). The number of apoptotic cells in the tail region (mainly muscle tissue) showed a non-linear absorbed dose-response, with a peak of deleterious effects around 250 mGy. Ten days after neutron exposure, the survival rate of the hatched larvae exposed to under 6 Gy was not different from that of the control group (around 99%), whereas the survival rate for the 15 Gy exposed group was around 80%. The LD_{50} was 0.53 Gy.

Total absorbed dose, absorbed dose rate and the type of radiation influence the effects of ionizing radiation. However, it is difficult to imagine a class of radiation exposure that is more complex in terms of its radiation fields (range of particle types and energies) and more challenging in terms of dose assessment than that presented by the radiation environment of space (Dietze et al., 2013). To account for the different effectiveness of radiation, radiation weighting factors have been recommended for humans by the International Commission for Radiological Protection in Publication 92 (ICRP, 2003) and specified for astronauts in Publication 123 (Dietze et al., 2013). Calculations made for neutrons in the energy range of 10^{-9}–10^{5} MeV indicate that the highest weighting factors are encountered at around 1 MeV (Dietze et al., 2013). While no similar weighting factors are proposed for neutrons in non-human species (Higley et al., 2021), this aligns with the higher lethality rates observed in zebrafish (*Danio rerio*) embryos compared to photon radiation, which were 10-fold higher for 1 MeV fission neutrons and 2.5-fold higher for p (18 MeV) Be cyclotron-generated fast neutrons (3.5 MeV) (Szabó et al., 2018).

Current technological developments do not allow to reproduce the whole spectrum of secondary particles produced inside the spacecraft. However, an increasing number of particle accelerator facilities are used as ground-based analogues for biology experiments and offer the opportunity to determine the relative contribution of individual secondary particles to observed biological effects. In this work, neutron exposure was performed at the ASNR (French Authority for Nuclear Safety and Radiation Protection) using the AMANDE particle accelerator. Located at the nuclear research site in Cadarache (France), AMANDE is a 2 MV tandem electrostatic accelerator that produces monoenergetic neutron fields of reference between 8 keV and 20 MeV. These fields are of primary interest for radiological protection, neutron metrology and nuclear physics (Gressier et al., 2003).

In the present study, the effect of secondary neutrons produced after the interaction of cosmic radiation with spacecraft shielding was investigated using the European sea bass *(Dicentrarchus labrax)* embryo, chosen as a candidate aquaculture fish species. The biological endpoints studied were the embryonic development (hatching rate), DNA damage (SSBs, DSBs and alkali-labile sites) and the histology of newly hatched larvae. Two experiments were performed over 2–3 days, enabling to monitor embryonic development until hatching. In the first experiment, exposure conditions were designed to mimic fish embryonic exposure in a low Earth orbiting context, such as a mission to the ISS, while the second experiment simulated exposure of a realistic Moon mission trajectory. Given that the applied dose rates are close to the derived consideration reference levels for fish (42-417 μGy h^{-1}), within which there is likely to be some chance of deleterious effects of ionizing radiation (ICRP, 2008), we expect limited effect of neutron on DNA damage and development of the fish early life stages.

2 Materials and methods

2.1 Aquaculture fish embryo fertilization, transportation and exposure design

European sea bass eggs were produced at the Ifremer aquaculture laboratory (Palavas-les-Flots, France) following the protocol described by Przybyla et al. (2023). Several thousand eggs were deposited into an incubator for 20 h. European seabass eggs (size ≈ 1.1 mm) are transparent and buoyant when alive. Small groups of 20 eggs were taken from the surface of the incubator to visually check their viability (binocular microscope Motic-w10X20) and then placed in the experimental containers, successively, until reaching the final number of 100 eggs per container (6 cm wide, 500 mL volume). Three experimental groups were created: (i) the group exposed to neutrons at ASNR's AMANDE facility, consisting of a triplicate of containers dedicated to the hatching rate assessment, one container for DNA damage analysis and one container for histological analysis; (ii) the non-exposed control group, consisting of the same number of containers kept at ASNR; and (iii) the standard group, consisting of a triplicate of containers kept at the Ifremer aquaculture facilities to assess only the hatching rate in an optimal aquaculture environment (without transport to the experimental site at ASNR).

The "exposed" and "control" groups were transported by car in a thermoregulated box maintained at 16.0°C ± 0.4°C from the Ifremer laboratory to the ASNR laboratory (200 km, 2 h 15 min. Containers were placed in large glass aquaria filled with water, allowing temperature regulation via a secondary thermoregulation circuit during exposure. Since fish embryo development is temperature-dependent, special attention was given to maintaining consistent water temperatures across all sites and groups. For all experiments and groups, water temperature was maintained at 16.10°C ± 0.1°C. The oxygen level measured inside the embryo containers never dropped below 92.3% of water saturation.

2.2 Neutron exposure

Neutron exposure was carried out at ASNR's AMANDE facility during working hours, with daily interruptions to take measurements or collect samples. The two exposure experiments were conducted separately in different dates under identical water temperature conditions and followed the same methods for fertilization, transport and egg distribution. Fertilized embryos were exposed to neutrons until hatching from 28 h post-fertilization (hpf) for ISS mission simulation, at 48-hpf for the Lunar journey simulation (Figure 1).

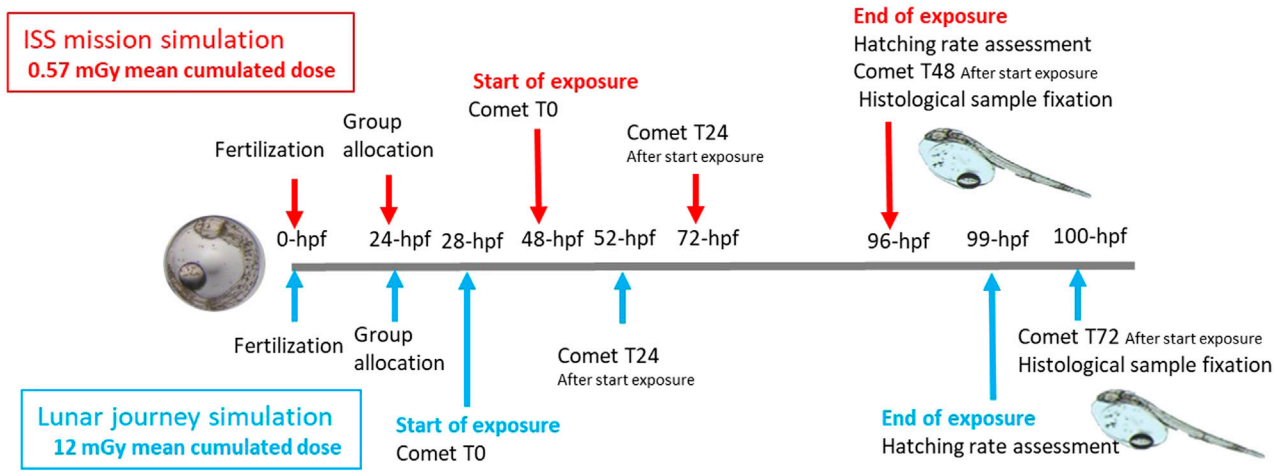

FIGURE 1
Exposure sampling timeline for the ISS-type experiment (mean cumulated dose and dose rate of 0.57 mGy and 16.7 μGy h^{-1}, respectively - red) and lunar mission experiment (mean cumulated dose and dose rate of 12 mGy and 585 μGy h^{-1}, respectively - blue).

2.3 Experiment 1: ISS-type exposure

2.3.1 Experimental design

The front glass wall of the aquarium containing the fish embryos in the small containers was positioned 188 cm from the accelerator beam's starting point (Figure 2). Inside the aquarium, a line of five submerged containers holding embryos was positioned in front of the particle accelerator beam. Particular attention was given to aligning the neutron beam with the embryo's waterline to ensure dose homogeneity. This line of containers on a single row was designated for DNA damage/histology analysis (container No. 1), hatching rate assessment (containers No. 2-3-4) and temperature sensor (container No. 5). The centers of the containers were positioned 4.5 cm from the aquarium wall.

2.3.2 Neutron dose and dose rate choice

For the ISS-type exposure, measurements performed by Smith et al. (2013) in the ISS were used. These measurements showed that the neutron spectra in the station presented two peaks at 1 MeV and 30 Mev, with a preponderance of the 1 MeV peak. The maximal dose rate measured was 378 μGy d^{-1} (16 μGy h^{-1}).

2.3.3 Exposure in AMANDE's facility

Given that the AMANDE facility provides mono-energetic neutrons, an energy of 1.2 MeV was chosen to mimic the neutron exposure conditions at the ISS. This energy is the reference derived from the standard ISO8529-1 (2021) and aligns with the spectra measured in Smith et al. (2013), which indicated a strong peak around 1 MeV. The energy was produced by directing a 2037 keV proton beam at a 780 μg cm^{-2} tritium target. A mean dose rate of 16.7 μGy h^{-1} per container was absorbed by the sea bass eggs. This exposure was provided over 34.2 h of irradiation (distributed across 47.6 h), which allowed to monitor the neutron effect on embryonic development. The mean total absorbed dose was 0.57 mGy. Absorbed doses and dose rates were also calculated for each endpoint (Supplementary Tables S1 and S2).

2.4 Experiment 2: lunar journey scenario

2.4.1 Experimental design

The front glass wall of the aquarium was positioned 90 cm from the accelerator beam's starting point (Figure 3A). In this lunar

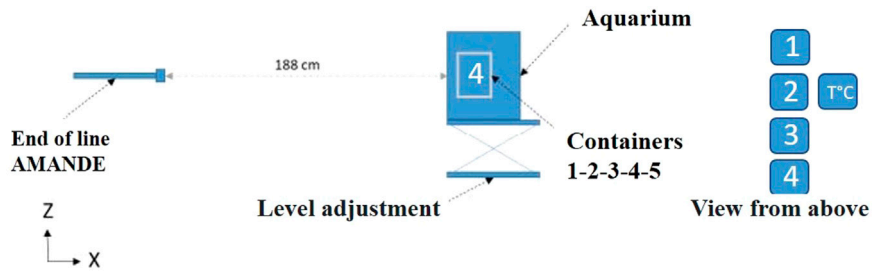

FIGURE 2
Cross-section of the AMANDE particle accelerator configuration for the ISS-type exposure experiment (1.2 MeV neutrons, mean dose rate of 16.7 μGy h^{-1}, mean total dose 0.57 mGy) and the position of the European sea bass embryo containers in the glass aquarium (n = 100 embryos/container). 1 - sea bass eggs dedicated to DNA damage/histological analyses; 2, 3, 4 - sea bass eggs for hatching rate assessment; 5 - temperature sensor.

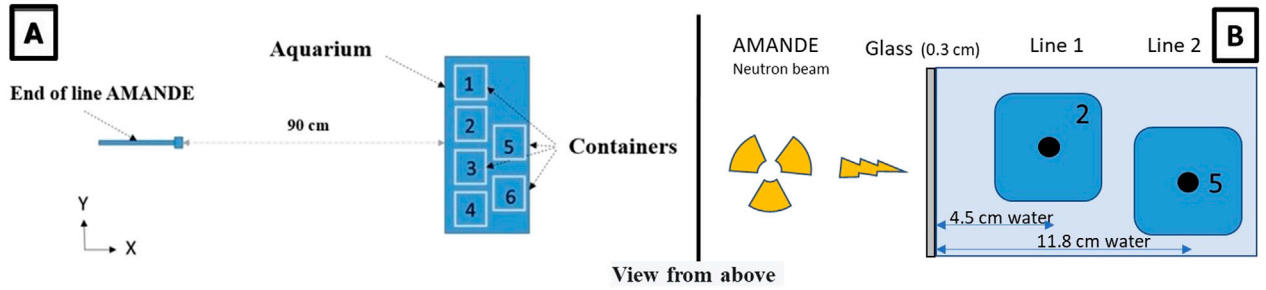

FIGURE 3
(A) View from above of the irradiation design for the lunar journey simulation experiment (20 MeV neutrons, mean dose rate of 585 μGy h^{-1}, mean cumulative dose 12 mGy) and the position of European sea bass embryo containers in the glass aquarium (n = 100 embryos/container). 1 - sea bass eggs dedicated to DNA damage analysis; 2, 3, 4 - sea bass eggs dedicated to hatching rate assessment; 5 - sea bass eggs for histological analyses; 6 - temperature sensor. **(B)** Distance traveled by neutrons through the aquarium glass wall into the water, depending on the container position (example shown for containers No. 2 and No. 5).

journey experiment, we separated the DNA damage and histology groups which led to creating a second row of embryo samples in the aquarium. The positioning of the first line of containers was the same as in the ISS-type experiment with centers located 4.5 cm from the aquarium glass. Due to neutron radiation passing through a thicker water layer to reach the second row, the cumulative neutron irradiation dose for embryos dedicated to histological analysis (container No. 5) was lower than that of the first row (See Supplementary Table S5). The center of the water temperature sensor (container No. 5; Figure 3B) and water temperature sensor were located at 11.8 cm from the aquarium glass.

2.4.2 Neutron dose and dose rates: simulation of the exposure during the lunar journey

The provisional trajectory of the lunar mission of the canceled ESA Heracles mission was used as a case study for this experiment. The characterization of secondary neutrons resulting from the interactions of high-energy particles (mainly protons) with the shielding was performed in terms of fluence integrated over the duration of the mission (expressed in neutrons. cm^{-2}) and absorbed dose. Proton spectra, which are important input data, were derived from two sources of protons: protons trapped in the Van Allen belt (3 days of exposure; Figure 4) and protons originating from the solar wind (5 days of exposure; Figure 4). Initial spectra for these two proton sources were computed using OMERE 5.6© software (https://www.trad.fr/spatial/logiciel-omere/). These spectra were then used as input data for the MONTE CARLO simulation toolkit Geant4 version 11.0.0 software (Agostinelli et al., 2003; Allison et al., 2016). Geant4, based on the interaction probabilities of particles with matter, allows the transport of particles through matter and to calculate the production of secondary particles as well as energy deposits like any Monte Carlo code. Geant4 was suitable for this study because it includes physical models adapted to the production and transport of secondary neutrons. Indeed, these physical models have been validated for secondary neutron yields in proton therapy applications for 113 and 256 MeV protons (Arce et al., 2021). For each proton source, protons were generated at the surface of an aluminum sphere 3.7 mm thick and 300 mm in radius, representing the shielding, and filled with water to mimic the fish's living environment. The assumed shielding thickness, which is still

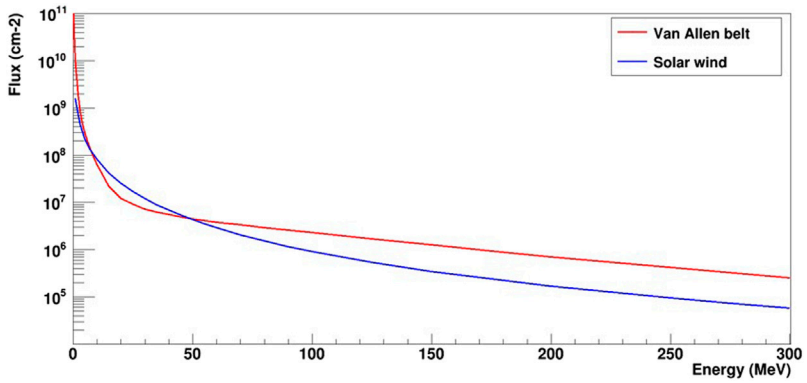

FIGURE 4
Flux of protons from the Van Allen belt (in red, 3 days of flight) and the solar wind (in blue, 5 days of flight).

in the design phase, represents a scenario that maximizes the impact of ionizing radiation in terms of dosimetry, which remains suitable for radiation protection. The actual shielding will certainly be thicker, making this experimental design an oversized extreme case in terms of exposure. The results obtained for 1.5 10^9 protons were then normalized to the actual fluence of the mission's total duration.

As expected, the main contribution to the production of secondary neutrons during the mission comes from the radiative environment of the Van Allen belt. With the assumptions made in the simulation, the total flux for the Van Allen belt was 5.05 10^8 cm^{-2}, whereas the flux from the solar wind was 1.84 10^7 cm^{-2}. This corresponds to absorbed doses of 24.5 mGy for the Van Allen belt and 0.9 mGy for the rest of the mission. Thus, the total secondary neutron absorbed dose for the 8-day lunar mission was 25.4 mGy, (corresponding to a dose rate of 130 μGy h^{-1}). It is possible to characterize the secondary neutron spectra for each proton source as shown in Figure 5. These spectra were normalized to the total flux expected during the mission. The mean energies of the secondary neutron spectra were 30 and 24 MeV for the Van Allen belt and solar wind origins, respectively.

2.4.3 Exposure in AMANDE facility

To expose the sea bass eggs to a neutron configuration corresponding to the simulated lunar mission, a series of calculations and assumptions were required with the AMANDE facility. First, as the AMANDE facility provides mono-energetic neutrons, the highest neutron energy available—20 MeV—was chosen to approximate the mean energies of the simulated secondary neutron spectra (30 and 24 MeV). Given that the neutron weighting factor at 20 MeV is higher than at 24 and 30 MeV (Supplementary Table S3), the choice of this energy potentially leads to more severe biological effects, ensuring a conservative toxicity assessment. Second, the total simulated neutron fluence (5.2 10^8 cm^{-2}) was the target nominal neutron fluence to be achieved at the AMANDE facility. A prior measurement of neutron fluence at the facility was performed using a reference long counter (Gressier et al., 2014) to determine the irradiation time required at 20 MeV to achieve this fluence. The required irradiation time was of 20.5 h, distributed over 4 days of irradiation (Supplementary Table S4). After verifying the experimental neutron characteristics, adjusted dose and dose rate were calculated to account for the presence of deuterium implanted in the target over time, which produces neutrons of 7 MeV (Supplementary Information). Finally, the mean experimental neutron dose and dose rate absorbed by the fish embryos were 12 mGy and 585 μGy h^{-1}, respectively. As in the ISS-type experiment, average doses and dose rates were calculated for each endpoint (Supplementary Tables S4 and S5). It must be underlined that although this dose is lower than the simulated one (25.6 mGy), it accounts for the presence of 7 MeV neutrons, which are more deleterious than 20 MeV neutrons, as detailed in the Supplementary Information file. Furthermore, as the neutron dose was distributed over 20.5 h instead of 8 days for a lunar mission, the resulting experimental dose rate (585 μGy h^{-1}) was higher than the simulated one (130 μGy h^{-1}). These conditions remain conservative in terms of toxicity evaluation.

2.5 Hatching rate assessment

The hatching rate was assessed after samples were filtered with a 700-μm mesh and visually analyzed to determine the number of newly hatched larvae. The same operator and binocular microscope were used for all counts to ensure consistency. The percentage of hatched fish was calculated based on the number of hatched eggs and the sample size (Przybyla et al., 2020).

2.6 Alkaline comet assay

Following the exposure of European sea bass eggs in the AMANDE facility, DNA damage was analyzed in embryos and larvae at 0 h (48 hpf), 24 h (72 hpf) and 48 h (96 hpf) after the start of neutron exposure in experiment 1, and at 0 h (28 hpf), 24 h (52 hpf) and 72 h (100 hpf) after the start of neutron exposure in experiment 2.

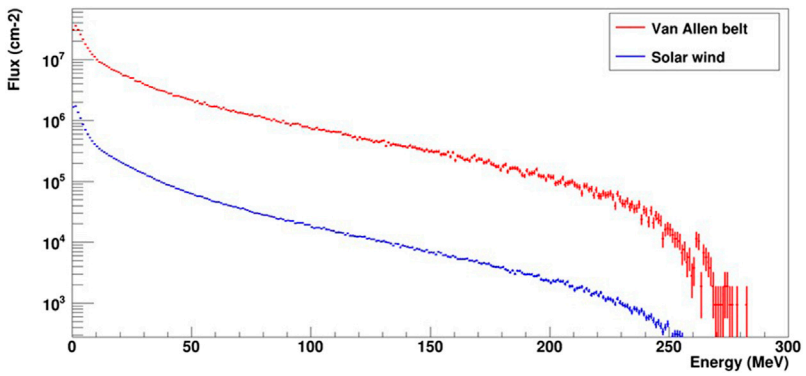

FIGURE 5
Flux of secondary neutrons produced over the entire mission duration by protons from the Van Allen belt (in red, 3 days of flight) and the solar wind (in blue, 5 days of flight).

The control groups (non-exposed, kept in the AMANDE facility) were analyzed at the same times.

The method used to measure DNA damages is the comet assay, which has been developed over the past 30 years (Collins, 2004). In this method, the final step consists in analyzing images resembling a comet, with a head representing the nucleus and a tail mainly consisting of single-stranded DNA that has migrated out from the cell nucleus. The magnitude of the comet's DNA-tail provides information about the extent of DNA lesions in the cell. The comet assay descriptor used in this experiment is the tail moment (the product of percentage of DNA in the tail and of tail length), which is one of the most widely used descriptors (Møller et al., 2014).

The alkaline comet assay, which detects DNA strand breaks (single- and double-strand breaks, as well as alkali-labile sites), was applied to European sea bass embryos and larvae. For 24 h and 48 h exposure times (non-hatched eggs), 3 to 5 pools of 4–10 eggs were used. In the case of larvae (72 h exposure time), the analysis was performed on four to six individual larvae. Embryos and larvae were kept on ice in seawater prior to the dissociation protocols. Cell dissociation was then performed using a pestle (Dutscher, 947827, France) in a PBS solution (100 mM phosphate-buffered saline) by mechanical homogenization.

The alkaline comet assay was conducted according to the procedure of Bourrachot et al. (2014) and MIRCA recommendations (Møller et al., 2020). Cells were stained with SYBR Gold diluted 1:10 (Invitrogen, S11494, United Kingdom), and one hundred nucleoids per slide were analyzed at ×400 magnification under a fluorescence microscope (Nikon Eclipse E600) equipped with a 515–560 nm excitation filter. Comet figures were analyzed using Comet IV software (Perceptive Instruments, United Kingdom). Two replicate slides were prepared per sample.

2.7 Histological analysis

European sea bass larvae (n = 5) were sampled from the exposed and control groups at 96 hpf in experiment 1 and at 100 hpf in experiment 2 (Figure 5), fixed in buffered paraformaldehyde (pH = 7.2) and stored at 4°C overnight. The following day, larvae were dehydrated using a graded series of ethanol and stored in 70% ethanol at 4°C until further processing. After dehydration, larvae were embedded in paraffin using an automatic tissue processor (STP120, Myr, France). Paraffin blocks were then prepared and cut into serial sagittal sections (3 µm thick) with an automatic microtome (Leica, RM 2235RT, United States). Paraffin sections were kept at 37°C overnight. Subsequently, samples were deparaffinized using a graded series of xylene substitute and stained with hematoxylin and eosin for general micromorphological observations. Histological preparations were observed under a microscope equipped with a camera (Leica, DM6 B, Germany). Tissue and cell integrity observations were carried out in three different section areas per organ and larva.

2.8 Statistical analyses

As the hatching rate data were expressed in percentages and close to the extremes [0; 1], a statistical analysis was performed with a converted value using $y = arc\sin\sqrt{x}$. The transformed data were subjected to one-way analysis of variance (ANOVA). GraphPad Prism 9.0 software (Dotmatics, Boston, Massachusetts, United States) was used for statistical analyses. Homogeneity of variance was tested using Fisher's test and the normality of distribution was assessed using the Shapiro–Wilk test.

For the comet assay, all statistical analyses were implemented with the statistical computing software R 4.2.2 (2022 The R Foundation for Statistical Computing). Raw data of the individual nucleoid tail moment were used for the analysis. Tail moments equal to zero were considered artifacts of the image analysis. However, since they represent "true" zeros (i.e., cells with no or poor DNA damage), they were replaced, if necessary, by the smallest value observed on the slide. Data were then log transformed. To address the nested design of the comet assay, a linear mixed-effects model was constructed using the nlme package, with treatment as the fixed factor and replicates (slides) as the random factor. Then, random permutation tests were applied using the pgirmess package, with the number of permutations fixed at 2,000.

2.9 Ethic statement

The experiments conducted at Ifremer and ASNR-AMANDE were carried out in accordance with the recommendations of the European Union Ethical Guidelines and Directive 2010/63/EU on the protection of animals used for scientific purposes. The Ifremer Marine Experimental Platform of Palavas (PEMP) permit for animal experimentation E 34-192-006 and the site's regional ethics committee (CEEA36 - Occitanie Méditerranée, France) ensured adherence to handling rules by the scientific team.

3 Results

3.1 Hatching rates

Hatching for all groups and both exposure levels occurred during the night of the last day of the experiment, between 96–99 hpf. For the ISS-type exposure experiment, the neutron field was active when the first hatching occurred, and the young pre-larvae managed to escape from the chorion around 86 hpf. Only one dead and one malformed larvae were observed in the "standard" group during the ISS-Type experiment.

The hatching rates of the "control," "exposed" and "standard" groups are presented in Figure 6 and show no significant intra-group differences within each exposure level. The hatching rates from the ISS and lunar mission exposures cannot be compared because the fish embryos originated from different broodstock.

3.2 DNA damage

The time-course histograms of DNA damages assessed via the comet assay are presented in Figures 7, 8. For the ISS-type exposure

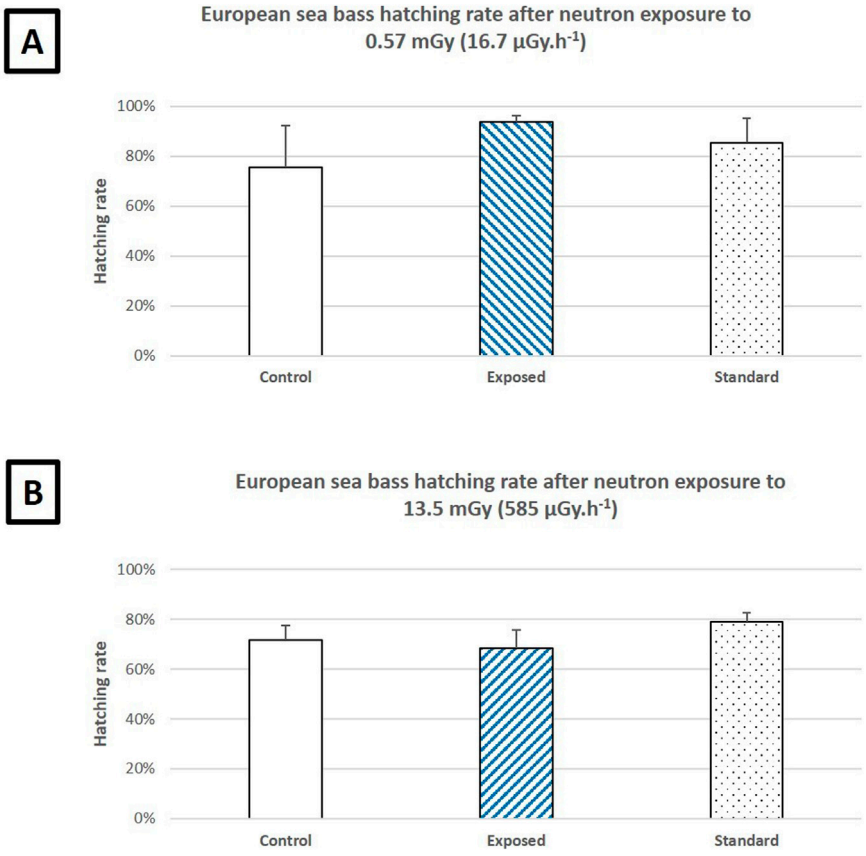

FIGURE 6
(A) Hatching rates of European sea bass embryos after a 34-h, 10-min neutron exposure simulating an ISS mission (1.2 MeV, 0.57 mGy, 16.7 µGy h^{-1}) compared to the control (non-exposed at AMANDE) and standard (non-exposed at Ifremer) groups. **(B)** Hatching rates of European sea bass embryos after a 20-h, 30-min neutron exposure simulating a lunar mission (7 and 20 MeV, 13.5 mGy, 585 µGy h^{-1}) compared to the control (non-exposed at AMANDE) and standard (non-exposed at Ifremer) groups. All groups were composed of 300 fertilized European seabass eggs divided in triplicate (3*100). Error bars represent the standard deviation. $P < 0.05$ (ANOVA).

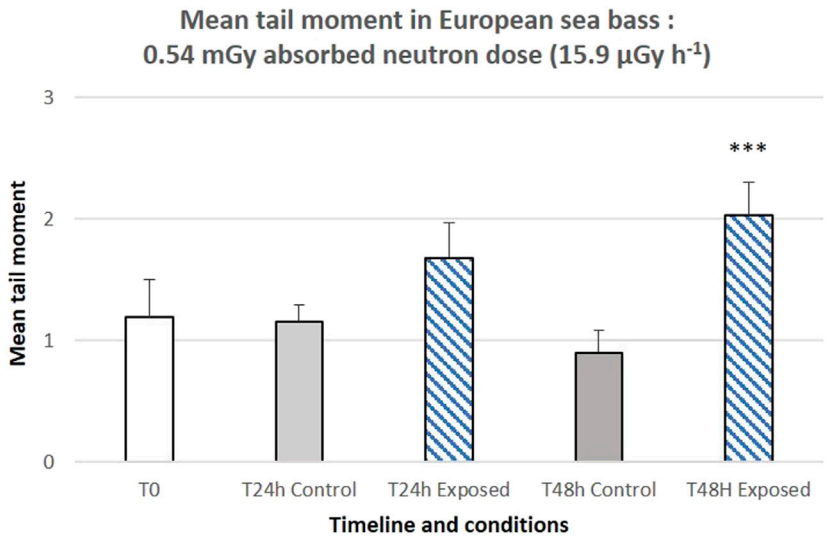

FIGURE 7
Genotoxicity (alkaline comet assay) induced after 24 h (left panel) or 48 h (right panel) of ISS-type exposure (1.2 MeV neutrons, 0.54 mGy and 15.9 µGy h^{-1} absorbed by eggs in containers dedicated to DNA damage analysis). 3 to 5 pools of 4–10 eggs were used. The bar represents the mean of 100 comets scored per slide. Error bars represent the standard error. ***: $p < 0.001$ (variance analysis with linear mixed-effects model).

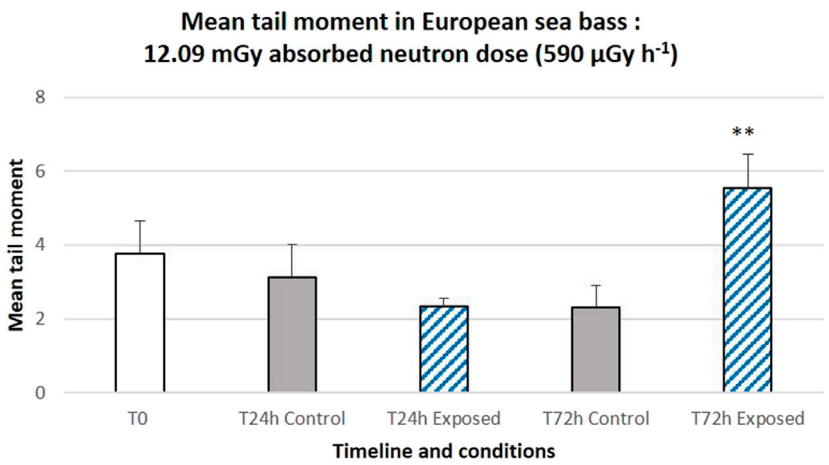

FIGURE 8
Genotoxicity (alkaline comet assay) induced after 24 h (left panel) or 72 h (right panel) of a lunar mission simulation exposure (7 MeV and 20 MeV neutrons, 12.09 mGy and 590 µGy h^{-1} absorbed by eggs in containers dedicated to DNA damage analysis). 3 to 5 pools of 4–10 eggs and four to six larvae were used, respectively for 24 h and 72 h exposure times. The bar represents the mean of 100 comets scored per slide. Error bars represent the standard error. **: $p < 0.01$ (variance analysis with linear mixed-effects model).

experiment, statistical analysis showed a significant increase in tail moments 48 h after the start of neutron exposure ($p = 0$) but not after 24 h ($p = 0.073$) (Figure 7).

Similarly, for the second exposure experiment, corresponding to a 12.09 mGy absorbed dose and a dose rate of 590 µGy h^{-1}, no significant increase in tail moments was observed at 24 h after the start of neutron exposure ($p = 0.38$), whereas a significant increase was observed at 72 h ($p = 0.002$) (Figure 8).

3.3 Histology

The overall organization of the various developing organs appeared to be maintained across all groups (Figure 9). For both the ISS and lunar mission simulation exposures, no signs of tissue or cellular damage were observed in any of the examined structures at 96 and 100 hpf, respectively, compared to the control groups. This applies to the brain, eyes, gills, notochord, muscle, digestive system

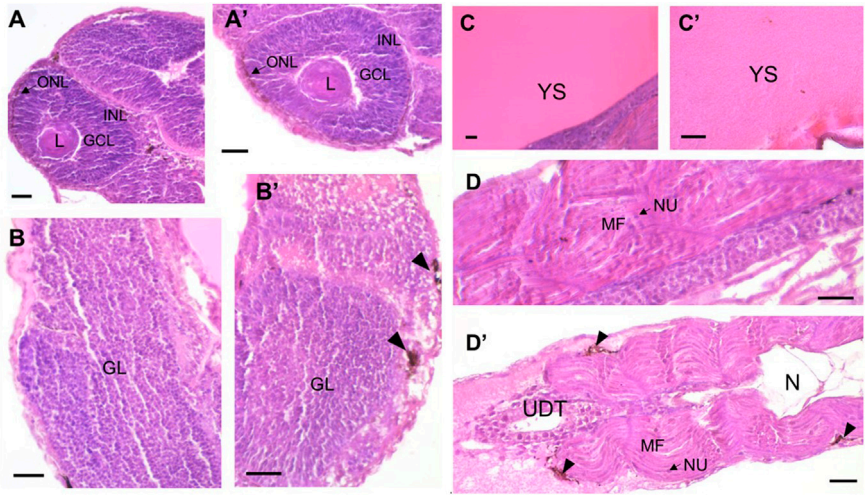

FIGURE 9
Longitudinal paraffin-embedded sections of European sea bass larvae at 96- and 100-h post-fertilization (hpf) for the ISS and lunar mission simulation experiments, respectively, showcasing the eye, brain, yolk sac and muscle of the control group (**(A–D)**, respectively) versus the group exposed to neutron radiation (**(A'–D')**, respectively). Panel **(A')** shows tissue after exposure of eggs in containers dedicated to histology analysis to 0.54 mGy and 15.9 µGy h^{-1} (ISS-type exposure); panels **(B'–D')** illustrate tissue after exposure of eggs in containers dedicated to histology analysis to 7.27 mGy and 355 µGy h^{-1} (lunar journey exposure). Sections were stained with hematoxylin and eosin. Anatomical features are labeled as follows: CGL, ganglion cell layer; GL, granular layer; INL, inner nuclear layer; L, lens; MF, muscle fiber; N, notochord; NU, nucleus; ONL, outer nuclear layer; UDT, undifferentiated digestive tract; YS, yolk sac. Arrowheads indicate melano-macrophage centers (MMC). Scale bar: 25 µm.

and yolk sac. Although not statistically significant (One Way ANOVA, $P > 0.05$), the number of melano-macrophage centers (MMC) tended to be higher in the brain and muscle areas of the group exposed to 7.3 mGy neutron radiation compared to the control group (Figure 9D–D′).

4 Discussion

The fish embryos dedicated to hatching rate assessment during the ISS and lunar mission simulations were exposed to a dose of 0.57 mGy (at a mean dose rate of 16.7 μGy h^{-1}) and 13.5 mGy (at a mean dose rate of 659 μGy h^{-1}), respectively. No mortality or shift in the expected hatching date was observed under either exposure condition, contrary to observations in simulated microgravity tests on European sea bass where the hatching date was advanced by a few hours (Przybyla et al., 2023). Accelerated hatching has been observed in zebrafish embryos exposed to γ-radiation dose rates of 33 and 23,8 10^3 μGy h^{-1} from 3 hpf to 96 hpf (Gagnaire et al., 2015), medaka embryos until the germ-ring stage exposed at up to 5 Gy (at a very high dose rate of 5.4 10^7 μGy h^{-1}) of 2 MeV neutrons (Hyodo-Taguchi et al., 1973) and Hong Kong catfish (*Clarias fuscus*) exposed to fast neutrons at 54 Gy h^{-1} (Hyodo-Taguchi et al., 1973).

The ISS- and lunar mission-type exposure experiments were conducted with embryos originating from different broodstock. Neither exposure level had deleterious effects on hatching performance compared to the standard or control groups. Hypometabolic states in fish could be studied for long space journeys, as zebrafish in a hypometabolic state following anoxic conditions have demonstrated tolerance (80% survival) to a supralethal dose of 20 Gy γ radiation (Ghosh et al., 2017). Hypometabolism could play a role in the physiological energy balance of fish in response to radiation-type aggression. Comparative ionizing radiation exposure studies involving temperate and tropical fish embryos could provide valuable insights for selecting aquaculture candidate species less susceptible to damage during their embryonic and larval stages.

DNA integrity in human and wildlife genomes is continuously challenged by both endogenous and environmental mutagens. Ionizing radiation, one of the first environmental genotoxic agents identified, can induce a wide variety of DNA lesions, including single-strand breaks, double-strand breaks and oxidative lesions. Among these, DNA double-strand breaks are considered the most deleterious, as their inaccurate repair can lead to cell death or mutations.

Genotoxicity can be assessed using several methods, including the comet assay under alkaline conditions (pH > 13), which can detect single and double-stranded breaks, and alkali-labile sites (OCDE, 2016). Comet assay results presented in this study indicate that neutrons increase DNA alterations 48–72 h after the start of exposure. These DNA damages may result from neutron interactions with DNA or from transient strand breaks resulting from DNA excision repair.

Neutrons are highly energetic uncharged particles that induce, via secondary protons, more localized and structurally complex clusters of double-strand break than γ rays. Modelling tools for calculating radiation-induced DNA damages have shown the propensity of neutrons to inflict clusters of DNA lesions containing DSBs (Baiocco et al., 2016; Manalad et al., 2023), findings that have been experimentally validated (Thibaut et al., 2023). Several studies describe various DNA damages induced by neutron exposure, although fish models have been scarcely addressed. In medaka, increased micronuclei frequencies were reported in gills of fish irradiated with a neutron-γ-ray mixed field from ^{235}U-enriched U fuel at a dose rate of 0.4 mGy h^{-1}, mean energy of fission neutrons of 1.3 MeV (Zhang et al., 2016). These results are in accordance with DNA damages induced by gamma exposure in various fish species showing an induction of genotoxicity in embryo and larvae from 33 μGy h^{-1} (Adam-Guillermin et al., 2012; Gagnaire et al., 2015). For other biological models exposed to neutrons, an increase in micronuclei was observed in human lymphocytes 24 h after irradiation with 0.3 Gy (1.55 Gy h^{-1}) neutrons whose spectrum was close to the Hiroshima neutron spectrum (Wang et al., 2021), while DNA DSBs were induced at doses from 0.125 Gy after exposure to fast neutrons (29.8 MeV) at both high (24 Gy h^{-1}) and low (0.9 Gy h^{-1}) dose rates (Nair et al., 2019). In rat peripheral blood cells, DNA DSBs were also induced at low dose rates (0.028 mGy h^{-1}) after 30 days of exposure to with neutrons and γ rays (cumulative dose of 16.8 mGy) (Zhang et al., 2016). The frequencies of somatic mutation and recombination were increased in *Drosophila melanogaster* exposed to fast and thermal neutrons from the Triga Mark III reactor in Mexico at doses up to 0.84 Gy (Guzmán-Rincón et al., 2005).

These studies indicate that DNA damages may occur at low doses and dose rates of neutrons (from 16.8 mGy to 0.028 mGy h^{-1}), as detected using the very sensitive γ-H2AX biomarker for DNA DSB, which is in accordance with the results presented here showing DNA damages from 0.54 mGy (0.016 mGy h^{-1}).

Interestingly, in 96-hour-old larvae of *D. melanogaster* irradiated with neutrons, the frequencies of mutations were higher than in 72-hour-old larvae (Guzmán-Rincón et al., 2005), which aligns with our results of higher and significant DNA damages in older embryos and larvae. This late onset of DNA damage could be explained by higher cell turnover during earlier developmental stages, resulting in lower DNA damage, or by an accumulation of DNA damage in later developmental stages due to higher absorbed doses.

Histological examinations are widely acknowledged as a reliable method for assessing the health of organisms faced with environmental challenges (Schwaiger et al., 1997; Zhao et al., 2020). Health condition indices are generally divided into three categories according to the levels of biological organization: whole organism, tissue and cellular levels, each functioning on distinct timescales. Simpler levels of biological organization tend to respond more swiftly to environmental changes, whereas more complex levels require more time to demonstrate changes. These variations depend on the specific developmental stage, species and environmental conditions. Given that DNA damage was observed in larvae 72 h after exposure began, it is unclear whether alternations at histological levels could have been observed at later developmental stages or whether DNA SSBs, DSBs and alkali-labile sites were either repaired or eliminated through apoptosis. Furthermore, the different locations of the containers for DNA damage and histological analyses within the aquaria, and the resulting differences in the absorbed dose and dose rate—nearly half of the values in the case of the histology samples—may have also influenced the differences between the

DNA damage and histological results. Nonetheless, the observed tendency for an increased number of MMC in some organs of the exposed group of experiment 2 may suggest a physiological response to neutron exposure, given that MMC are considered reliable indicators of environmental stress, such as starvation, hypoxic conditions and chemical exposure (Agius and Roberts, 2003).

5 Conclusion

Despite primary DNA damages observed in both types of exposure after 48 and 72 h for ISS-type and lunar journey exposures, respectively, embryogenesis in European sea bass was not significantly altered, which may indicate that DNA damages were repaired or were not lethal. Although the larvae in this experiment are alive with normal behavior, further investigation is needed to determine the impact of neutron radiation on the integrity of cells, tissues and organs at later developmental stages, as well as its subsequent influence on overall fish growth performance and health. Alongside similarly positive results from previous experiments on the effects of launcher vibration, hypergravity and microgravity on aquaculture fish eggs, our results reinforce the suitability of aquatic organisms as candidates for integration into ecological life support systems beyond Earth, potentially contributing to space food production activities. Further studies might consider other exposures to primary and secondary particles, such as proton or alpha radiation generated in the cabin during a lunar mission. The promising results of the ground-based mono-parametric simulations in this study (neutrons) and in previous studies (rocket vibrations, hypergravity, microgravity) allow us to consider the study of the cumulative impact of these environmental parameters during a space mission through a proof-of-concept flight in order to describe the hatching and larval development of an aquaculture fish species either on the ISS or during a bio-mission to the Moon.

Data availability statement

The raw data supporting the conclusion of this article will be made available by the authors, without undue reservation.

Ethics statement

The animal study was approved by European Union Ethical Guidelines and Directive 2010/63/EU + Animal experimentation E 34-192-006 and the site's regional ethics committee (CEEA36 - Occitanie Méditerranée, France). The study was conducted in accordance with the local legislation and institutional requirements.

Author contributions

CP: Conceptualization, Formal Analysis, Funding acquisition, Investigation, Methodology, Project administration, Resources, Writing – original draft, Writing – review and editing. RB: Conceptualization, Investigation, Methodology, Resources, Writing – original draft, Writing – review and editing. HL: Methodology, Supervision, Writing – review and editing. GD: Conceptualization, Formal Analysis, Investigation, Methodology, Writing – review and editing. EM: Conceptualization, Formal Analysis, Investigation, Methodology, Resources, Writing – review and editing. SE: Formal Analysis, Investigation, Writing – review and editing. SL: Methodology, Writing – review and editing. IC: Formal Analysis, Writing – review and editing. MD: Conceptualization, Data curation, Formal Analysis, Investigation, Methodology, Supervision, Validation, Writing – original draft, Writing – review and editing. SH: Investigation, Methodology, Supervision, Validation, Writing – review and editing. NB: Investigation, Methodology, Validation, Writing – review and editing. YP: Conceptualization, Formal Analysis, Methodology, Validation, Writing – original draft, Writing – review and editing. CA-G: Conceptualization, Formal Analysis, Funding acquisition, Investigation, Methodology, Supervision, Validation, Writing – original draft, Writing – review and editing.

Funding

The author(s) declare that financial support was received for the research and/or publication of this article. The "CORAFE" project was funded by the French Space Agency CNES (contract: Aide à la Recherche no4800001161), the French National Institute for Ocean Science (MARBEC unit R120-03-DF), the joint research unit MARBEC and the French Authority for Nuclear Safety and Radiation Protection (ASNR).

Acknowledgments

The authors deeply thank the radiology expert group involved in the preliminary discussions around the exposure protocol: Nicolas Foray (National Institutes of Health and Medical Research-INSERM), Françoise Berezza (National Centre for Space Studies-CNES), Laurent Dusseau and Muriel Bernard (Space center of the University of Montpellier-CSUM). They also appreciate the fruitful exchanges during the project with Béatrice Gagnaire, Magali Floriani and François Vianna-Legros (French Authority for Nuclear Safety and Radiation Protection-ASNR). The author thanks Guillemette Gauquelin-Koch (CNES) for the recurring support to the Lunar Hatch program through the French space agency's research assistance call. And finally, all the people involved at Ifremer in the implementation and management of this space aquaculture project.

Conflict of interest

The authors declare that the research was conducted in the absence of any commercial or financial relationships that could be construed as a potential conflict of interest.

Generative AI statement

The author(s) declare that no Generative AI was used in the creation of this manuscript.

Publisher's note

All claims expressed in this article are solely those of the authors and do not necessarily represent those of their affiliated organizations, or those of the publisher, the editors and the reviewers. Any product that may be evaluated in this article, or claim that may be made by its manufacturer, is not guaranteed or endorsed by the publisher.

Supplementary material

The Supplementary Material for this article can be found online at: https://www.frontiersin.org/articles/10.3389/frspt.2025.1571592/full#supplementary-material

References

Adam-Guillermin, C., Pereira, S., Della-Vedova, C., Hinton, T., and Garnier-Laplace, J. (2012). Genotoxic and reprotoxic effects of tritium and external gamma irradiation on aquatic animals. *Rev. Environ. Contam. Toxicol.* 220, 67–103. doi:10.1007/978-1-4614-3414-6_3

Agius, C., and Roberts, R. J. (2003). Melano-macrophage centres and their role in fish pathology. *J. Fish Dis.* 26, 499–509. doi:10.1046/j.1365-2761.2003.00485.x

Agostinelli, S., Allison, J., Amako, K., Apostolakis, J., Araujo, H., Arce, P., et al. (2003). Geant4—a simulation toolkit. *Nucl. Instrum. Methods Phys. Res. Sect. A Accel. Spectrom. Detect. Assoc. Equip.* 506, 250–303. doi:10.1016/S0168-9002(03)01368-8

Allison, J., Amako, K., Apostolakis, J., Arce, P., Asai, M., Aso, T., et al. (2016). Recent developments in Geant4. *Nucl. Instrum. Methods Phys. Res. Sect. A Accel. Spectrom. Detect. Assoc. Equip.* 835, 186–225. doi:10.1016/j.nima.2016.06.125

Arce, P., Bolst, D., Bordage, M., Brown, J. M. C., Cirrone, P., Cortés-Giraldo, M. A., et al. (2021). Report on G4-med, a Geant4 benchmarking system for medical physics applications developed by the Geant4 medical simulation benchmarking group. *Med. Phys.* 48, 19–56. doi:10.1002/mp.14226

Baiocco, G., Barbieri, S., Babini, G., Morini, J., Alloni, D., Friedland, W., et al. (2016). The origin of neutron biological effectiveness as a function of energy. *Sci. Rep.* 6, 34033. doi:10.1038/srep34033

Bourrachot, S., Brion, F., Pereira, S., Floriani, M., Camilleri, V., Cavalié, I., et al. (2014). Effects of depleted uranium on the reproductive success and F1 generation survival of zebrafish *Danio rerio*. *Aquat. Toxicol.* 154, 1–11. doi:10.1016/j.aquatox.2014.04.018

Chancellor, J. C., Blue, R. S., Cengel, K. A., Aunon-Chancellor, S. M., Rubins, K. H., Katzgraber, H. G., et al. (2018). Limitations in predicting the space radiation health risk for exploration astronauts. *NPJ Microgravity* 4, 8. doi:10.1038/s41526-018-0043-2

Collins, A. R. (2004). The comet assay for DNA damage and repair: principles, applications, and limitations. *Mol. Biotechnol.* 26, 249–261. doi:10.1385/mb:26:3:249

Cooper, M., Perchonok, M., and Douglas, G. L. (2017). Initial assessment of the nutritional quality of the space food system over three years of ambient storage. *NPJ Microgravity* 3, 17. doi:10.1038/s41526-017-0022-z

Dietze, G., Bartlett, D., Cool, D., Cucinotta, F., Jia, X., McAulay, I., et al. (2013). ICRP publication 123: assessment of radiation exposure of astronauts in space. *ICRP Publ. 123 Ann. ICRP* 42, 1–339. doi:10.1016/j.icrp.2013.05.004

Douglas, G. L., Zwart, S. R., and Smith, S. M. (2020). Space food for thought: challenges and considerations for food and nutrition on exploration missions. *J. Nutr.* 150, 2242–2244. doi:10.1093/jn/nxaa188

Fisher, R., Baselet, B., Vermeesen, R., Moreels, M., Baatout, S., Rahiman, F., et al. (2020). Immunological changes during space travel: a ground-based evaluation of the impact of neutron dose rate on plasma cytokine levels in human whole blood cultures. *Front. Phys.* 8. doi:10.3389/fphy.2020.568124

Gagnaire, B., Cavalie, I., Pereira, S., Floriani, M., Dubourg, N., Camilleri, V., et al. (2015). External gamma irradiation-induced effects in early-life stages of zebrafish, *Danio rerio*. *Danio rerio Aquat. Toxicol.* 169, 69–78. doi:10.1016/j.aquatox.2015.10.005

Ghosh, S., Indracanti, N., Ray, J., and Kumar, I. (2017). Deep hypometabolic state mitigates radiation-induced lethality in zebrafish. *Biomed. Res. Clin. Prac.* 2. doi:10.15761/brcp.1000139

Gressier, V., Lacoste, V., Martin, A., and Pepino, M. (2014). Characterization of a measurement reference standard and neutron fluence determination method in IRSN monoenergetic neutron fields. *Metrologia* 51, 431–440. doi:10.1088/0026-1394/51/5/431

Gressier, V., Pelcot, G., Pochat, J. L., and Bolognese-Milstajn, T. (2003). New IRSN facilities for neutron production. *Nucl. Instrum. Methods Phys. Res. Sect. A Accel. Spectrom. Detect. Assoc. Equip.* 505, 370–373. doi:10.1016/S0168-9002(03)01099-4

Guzmán-Rincón, J., Delfín-Loya, A., Ureña-Núñez, F., Paredes, L. C., Zambrano-Achirica, F., and Graf, U. (2005). Genotoxicity of neutrons in *Drosophila melanogaster*. *Somat. Mutat. Recomb. Induc. by React. Neutrons Radiat. Res.* 164, 157–162. doi:10.1667/rr3405

Higley, K., Real, A., and Chambers, D. (2021). ICRP publication 148: radiation weighting for reference animals and plants. *Ann. ICRP* 50, 9–133. doi:10.1177/0146645319896548

Hyodo-Taguchi, Y., Etoh, H., and Egami, N. (1973). RBE of fast neutrons for inhibition of hatchability in fish embryos irradiated at different developmental stages. *Radiat. Res.* 53, 385–391. doi:10.2307/3573771

ICRP (2003). Relative biological effectiveness (RBE), quality factor (Q), and radiation weighting factor (wR). *Ann. ICRP* 33 (4), 1–121. doi:10.1016/s0146-6453(03)00024-1

ICRP (2008). Environmental Protection - the Concept and Use of Reference Animals and Plants. *ICRP Publication 108*. Ann. ICRP 38 (4–6).

Kuhne, W. W., Gersey, B. B., Wilkins, R., Wu, H., Wender, S. A., George, V., et al. (2009). Biological effects of high-energy neutrons measured *in vivo* using a vertebrate model. *Radiat. Res.* 172, 473–480. doi:10.1667/rr1556.1

Manalad, J., Montgomery, L., and Kildea, J. (2023). A study of indirect action's impact on simulated neutron-induced DNA damage. *Phys. Med. Biol.* 68, 075014. doi:10.1088/1361-6560/acc237

Møller, P., Azqueta, A., Boutet-Robinet, E., Koppen, G., Bonassi, S., Milić, M., et al. (2020). Minimum Information for Reporting on the Comet Assay (MIRCA): recommendations for describing comet assay procedures and results. *Nat. Protoc.* 15, 3817–3826. doi:10.1038/s41596-020-0398-1

Møller, P., Loft, S., Ersson, C., Koppen, G., Dusinska, M., and Collins, A. (2014). On the search for an intelligible comet assay descriptor. *Front. Genet.* 5, 217. doi:10.3389/fgene.2014.00217

Nair, S., Engelbrecht, M., Miles, X., Ndimba, R., Fisher, R., du Plessis, P., et al. (2019). The impact of dose rate on DNA double-strand break formation and repair in human lymphocytes exposed to fast neutron irradiation. *Int. J. Mol. Sci.* 20, 5350. doi:10.3390/ijms20215350

OCDE (2016). "Test No. 489: *in vivo* mammalian alkaline comet assay," in *OECD Guidelines for the Testing of Chemicals*. (Paris: OECD Publishing) doi:10.1787/9789264264885-en

Przybyla, C. (2021). Space aquaculture: prospects for raising aquatic vertebrates in a bioregenerative life-support system on a lunar base. *Front. Astronomy Space Sci.* 8. doi:10.3389/fspas.2021.699097

Przybyla, C., Bonnefoy, J., Paounov, R., Debiol, A., Dutto, G., Mansuy, E., et al. (2023). Embryogenesis of an aquaculture fish (*Dicentrarchus labrax*) under simulated altered gravity. *Front. Space Technol.* 4. doi:10.3389/frspt.2023.1240251

Przybyla, C., Dutto, G., Bernard, M., Rollin, B., Laurand, X., Averseng, J., et al. (2020). European sea bass (*Dicentrarchus labrax*) and meagre (Argyrosomus regius) fertilized egg resistance to a spacecraft launcher vibration qualifying test. *Aquac. Int.* 28, 2465–2479. doi:10.1007/s10499-020-00601-5

Schwaiger, J., Wanke, R., Adam, S., Pawert, M., Honnen, W., and Triebskorn, R. (1997). The use of histopathological indicators to evaluate contaminant-related stress in fish. *J. Aquatic Ecosyst. Stress Recovery* 6, 75–86. doi:10.1023/A:1008212000208

Shavers, M. R., Semones, E. J., Shurshakov, V., Dobynde, M., Sato, T., Komiyama, T., et al. (2024). Comparison of dose and risk estimates between ISS Partner Agencies for a 30-day lunar mission. *Med. Phys.* 34, 31–43. doi:10.1016/j.zemedi.2023.10.005

Smith, M. B., Akatov, Y., Andrews, H. R., Arkhangelsky, V., Chernykh, I. V., Ing, H., et al. (2013). Measurements of the neutron dose and energy spectrum on the International Space Station during expeditions ISS-16 to ISS-21. Radiat. *Prot. Dosimetry*. 153, 509–533. doi:10.1093/rpd/ncs129

Szabó, E. R., Reisz, Z., Polanek, R., Tőkés, T., Czifrus, S., Pesznyák, C., et al. (2018). A novel vertebrate system for the examination and direct comparison of the relative biological effectiveness for different radiation qualities and sources. *Int. J. Radiat. Biol.* 94, 985–995. doi:10.1080/09553002.2018.1511928

Thibaut, Y., Gonon, G., Martinez, J. S., Petit, M., Babut, R., Vaurijoux, A., et al. (2023). Experimental validation in a neutron exposure frame of the MINAS TIRITH for cell damage simulation. *Phys. Med. and Biol.* 68, 225008. doi:10.1088/1361-6560/ad043d

Verseux, C., Poulet, L., and de Vera, J. P. (2022). Editorial: bioregenerative life-support systems for crewed missions to the Moon and Mars. *Front. Astronomy Space Sci.* 9. doi:10.3389/fspas.2022.977364

Wang, Q., Lee, Y., Pujol-Canadell, M., Perrier, J. R., Smilenov, L., Harken, A., et al. (2021). Cytogenetic damage of human lymphocytes in humanized mice exposed to neutrons and X rays 24 h after exposure. *Cytogenet Genome Res.* 161, 352–361. doi:10.1159/000516529

Warden, D., and Bayazitoglu, Y. (2019). New comparative metric for evaluating spacecraft radiation shielding. *J. Spacecr. Rockets* 56, 1024–1038. doi:10.2514/1.A34360

Zabel, P., Bamsey, M., Schubert, D., and Tajmar, M. (2016). Review and analysis of over 40 years of space plant growth systems. *Life Sci. Space Res.* 10, 1–16. doi:10.1016/j.lssr.2016.06.004

Zeidler, C., Vrakking, V., Bamsey, M., Poulet, L., Zabel, P., Schubert, D., et al. (2017). Greenhouse module for space system: a lunar greenhouse design. *Open Agric.* 2, 116–132. doi:10.1515/opag-2017-0011

Zhang, J., He, Y., Shen, X., Jiang, D., Wang, Q., Liu, Q., et al. (2016). γ-H2AX responds to DNA damage induced by long-term exposure to combined low-dose-rate neutron and γ-ray radiation. *Mutat. Research/Genetic Toxicol. Environ. Mutagen.* 795, 36–40. doi:10.1016/j.mrgentox.2015.11.004

Zhao, L., Cui, C., Liu, Q., Sun, J., He, K., Adam, A. A., et al. (2020). Combined exposure to hypoxia and ammonia aggravated biological effects on glucose metabolism, oxidative stress, inflammation and apoptosis in largemouth bass (*Micropterus salmoides*). *Aquat. Toxicol.* 224, 105514. doi:10.1016/j.aquatox.2020.105514